이학석사 학위논문

Inter-annual variation in the southern limit of the YSBCW and its causes in summer

여름철 황해 저층냉수 남쪽한계의 연변화와 원인

2013년 8월

서울대학교 대학원

지구환경과학부

양희원

Abstract

Inter-annual variation in the southern limit of the YSBCW and its causes in summer

Hee Won, Yang

School of Earth and Environmental Sciences

The Graduate School

Seoul National University

The Yellow Sea Bottom Cold Water (YSBCW) is defined as the water mass with temperature less than 10℃, which is found below the thermocline in summer. This study identifies the southern limit of the YSBCW and investigates the mechanisms driving the inter-annual variability of the YSBCW.

The observed temperature in August by the National Fisheries Research & Development (NFRDI) during the last 30 years is analyzed. The southern limit is defined as the distance of 10℃ isothermal line from the observation line 307 by NFRDI. The southern limit shows a pronounced inter-annual variability. To complement the observation-based analysis, we also use a numerical model that captures the observed variation of the southern limit of YSBCW fairly well.

In both the model and observation, February SST is highly correlated with the southern limit in August. This result suggests that cold sea surface temperature is associated with increased southern limit in the following summer.

We also find that the southern limit is more extended to the south in August than in June in some years. This is thought to be due to the influence of the summer southerly winds that drive the southward extension of the August southern limit near the bottom.

Winter winds together with cold air temperature induce strong heat loss at the sea surface. The resulting cold SST influences the southern limit in the following summer.

The other factors affecting the southern limit variation besides the above factors include previous year's bottom water temperature. A comparison between 75m temperature in October representing previous year's oceanic condition and SST in February shows a positive correlation in both the model and observation.

Keywords – Yellow Sea, temperature, Yellow Sea Bottom Cold Water, inter-annual variation, sea surface temperature, air temperature, wind stress

Student Number : 2011-23266

List of Contents

List of Figures

1. Introduction

The Yellow Sea (YS), which is located between Korea and China, is a shallow and semi enclosed marginal sea (Figure 1). Adjoining rivers bring sediments rich in nutrients to the YS. High primary productivity, abundant marine life and dominating monsoon conditions demonstrate the importance of the YS in perspectives of the marine ecosystem and geography [Teng et al., 2005]. Shallow depth (less than 100m) and pronounced seasonal change in the YS cause large variation of the sea water temperature.

Strong northerly wind drives deep convection in winter, resulting in vertically well mixed waters from the surface to the bottom during winter (Figure 2 a). This vertical temperature structure can be observed until April (Figure 2 b). On the other hand, increased solar radiation drives strong stratification in summer. Because the strong stratification prevents vertical mixing between sea surface and bottom in summer, cold water formed in winter keep its temperature beneath the stratified thermocline (Figure 2c and d). This cold water is called the Yellow Sea Bottom Cold Water (YSBCW) [Guan, 1963; Hur et al., 1999; Kim et al., 1999; Hu et al., 2004; Zhang et al., 2008; Park et al., 2011].

Previous studies have already explored some aspects of this unique water mass. Recently, inter-annual or long-term changes of sea water temperature in the YS have been studied. Park et al., (2011) reported that changes in atmosphere forcing are strongly correlated with the variability of the YSBCW temperature. Hu et al.

(2004) examined the inter-annual variability of the YSBCW temperature and its driving mechanisms in the southern YS. Seasonal and long-term variation of observed temperature was studied by Zhang et al. (2008).

Previous studies suggested that winter air temperature may affect variability of the YSBCW temperature [Guan, 1963; Kim et al., 1999; Park et al., 2011]. There are two different views regarding the role of the winter wind. Northerly winds can lead to large heat loss [Kim et al., 1999]. On the other hand, upwind flow of warm and salty water caused by the northerly monsoonal winds can affect the YSBCW in the southern YS [Hsueh and Yuan, 1997].

Recently southward migration of the YSBCW in summer has been reported. Zhang et al. (2008) showed that the cold bottom water moves from the north to the central area of the YS during the summer based on short time observed data. Jacobs et al. (2000) revealed that southeasterly summer monsoon generates a southward flow of the bottom layer, using a numerical model. The seasonal migration of the YSBCW has a large impact on primary products and marine habitats due to dramatic change of water temperature in the southern YS [Wang et al., 2003].

However the inter-annual variation of the southern limit of the YSBCW and its driving mechanisms are poorly known. The purpose of this paper is to investigate the inter-annual variations of the southern limit of the YSBCW and its causes using long-term observations and a numerical model.

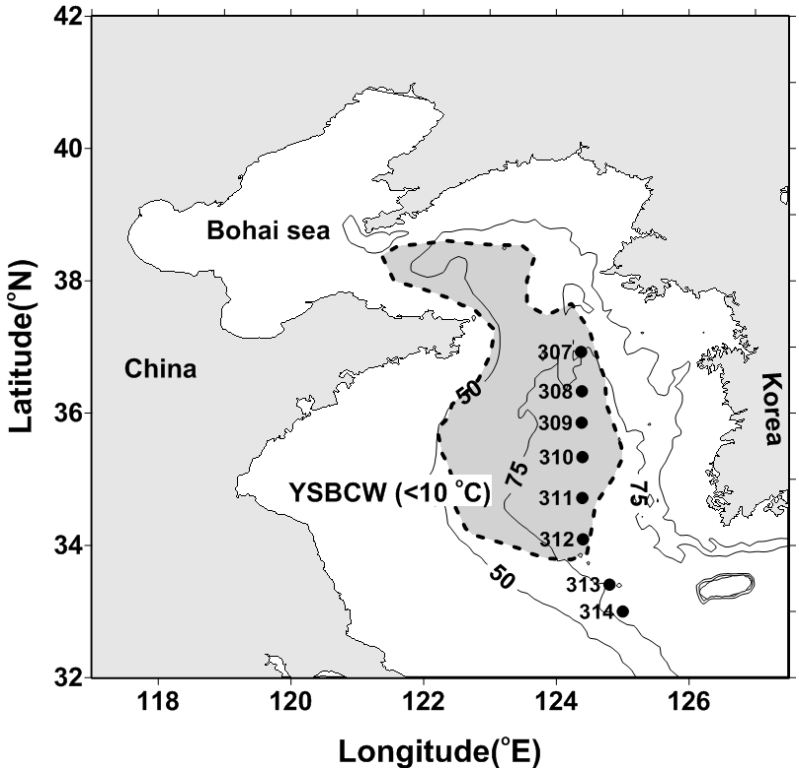

Figure 1. Bathymetric map of the YS and schematic diagrams of the YSBCW (gray) by model result. Numbers represent observation line routinely observed by the National Fisheries Research & Development Institute.

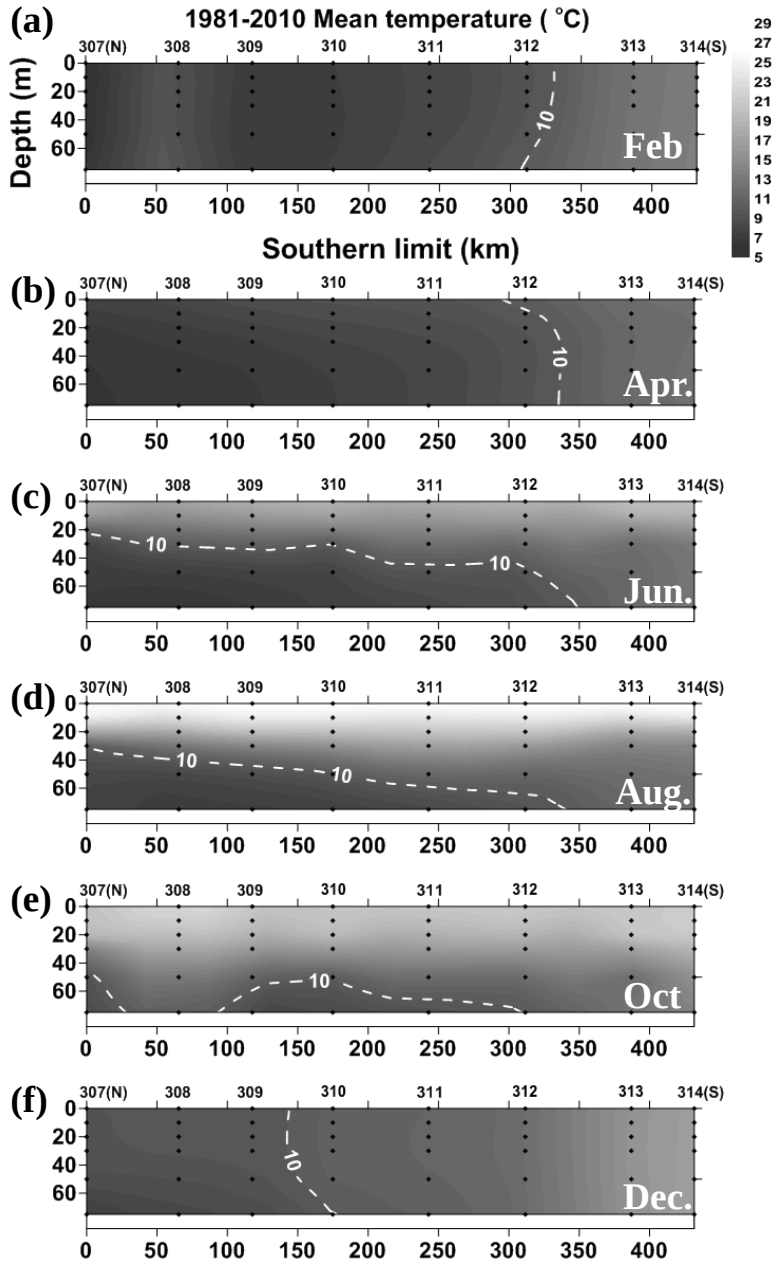

Figure 2. Mean meridional section of temperature along the observation stations of Figure 1 in (a) February (b) April (c) June (d) August (e) October (f) December from 1981 to 2010.

2. Data and methodology

The observed temperatures by the National Fisheries Research and Development Institute (NFRDI) during the last 30 years (1981-2010) were analyzed. Temperature data has been routinely observed bimonthly at the standard depths in the sea around Korean Peninsula. Most offshore stations of each observed line which correspond to deep trough in the YS were selected (filled circles in Figure 1) to study the variation of the southern limit of the YSBCW in August. Number at each station represents observed line by NFRDI. Temperatures observed at a depth of 75 m were analyzed for bottom water at all stations. Mean temperature distributions at 75 m in each month are shown in Appendix Figure 1. Sea surface temperature at same stations in February was used to examine the correlation between the southern limit of the YSBCW and the winter water temperature.

Observed data might have many limitations in quantify the variation of the YSBCW and the relation with its causes due to observation errors and coarse resolutions in time and space. Thus, we also use a numerical model to complement the observation-based analysis.

The Regional Ocean modeling System (ROMS), which is a three dimensional ocean circulation model, was used for this study. The model domain is from 18.5°N to 48.5°N and from 117.5°E to 154.5°E which includes the YS, the East China Sea, the East Sea and the Northwestern Pacific. The horizontal grid has a resolution of 0.1° with 20 vertical levels. The open boundary data of the model were provided from a regional northwest Pacific (NWP) model [Cho et al., 2009]. The NWP

model is nested within a data assimilative global model known as Estimating the Circulation and Climate of the Ocean (ECCO; www.ecco-group.org). The initial values for temperature, salinity, velocity, and sea surface height are obtained from the NWP model [Cho et al., 2009]. The model is run from 1980, January to 2010, December. The monthly mean values from the ECMWF reanalysis data were used as the surface forcing and bulk-flux formulae [Fairall et al., 1996] were adapted. Tidal forcing with ten major tidal components was applied [Egbert and Erofeeva, 2002]. Vertical mixing was calculated by the Mellor-Yamada turbulence closure scheme [Mellor and Yamada, 1974]. The horizontal viscosity coefficient was set to 300 m^2/s. Further details on the model can be found in Cho et al. (2009, 2013). We analyze the temperature selected from model grids corresponding to the observation. Monthly mean bottom temperature of model results shows well the evolution of the YSBCW in the whole area (Figure 3), whereas the observation shows limited feature (Appendix Figure 1).

To relate the YSBCW inter-annual variations with the change in atmospheric conditions, we use monthly mean air temperature and wind stress from the ECMWF reanalysis during the last 30 years of 1981- 2010. As winter air temperature, we average the December, January and February air-temperature over a domain bounded by 33°N, 42°N, 117°E, and 127°E (Appendix Figure 2). Winter wind speed and summer wind stress were calculated using the V (north-south) component wind speed spatially averaged from 30°N to 42°N and from 117°E to 127°E in December, January and February and in June, July and August, respectively (Appendix Figure 3).

To identify the previous year's oceanic condition influencing the YSBCW

variability, the 75m temperature in October of the observed data and model result were analyzed. Both data are spatial mean temperature at the same stations in Figure 1.

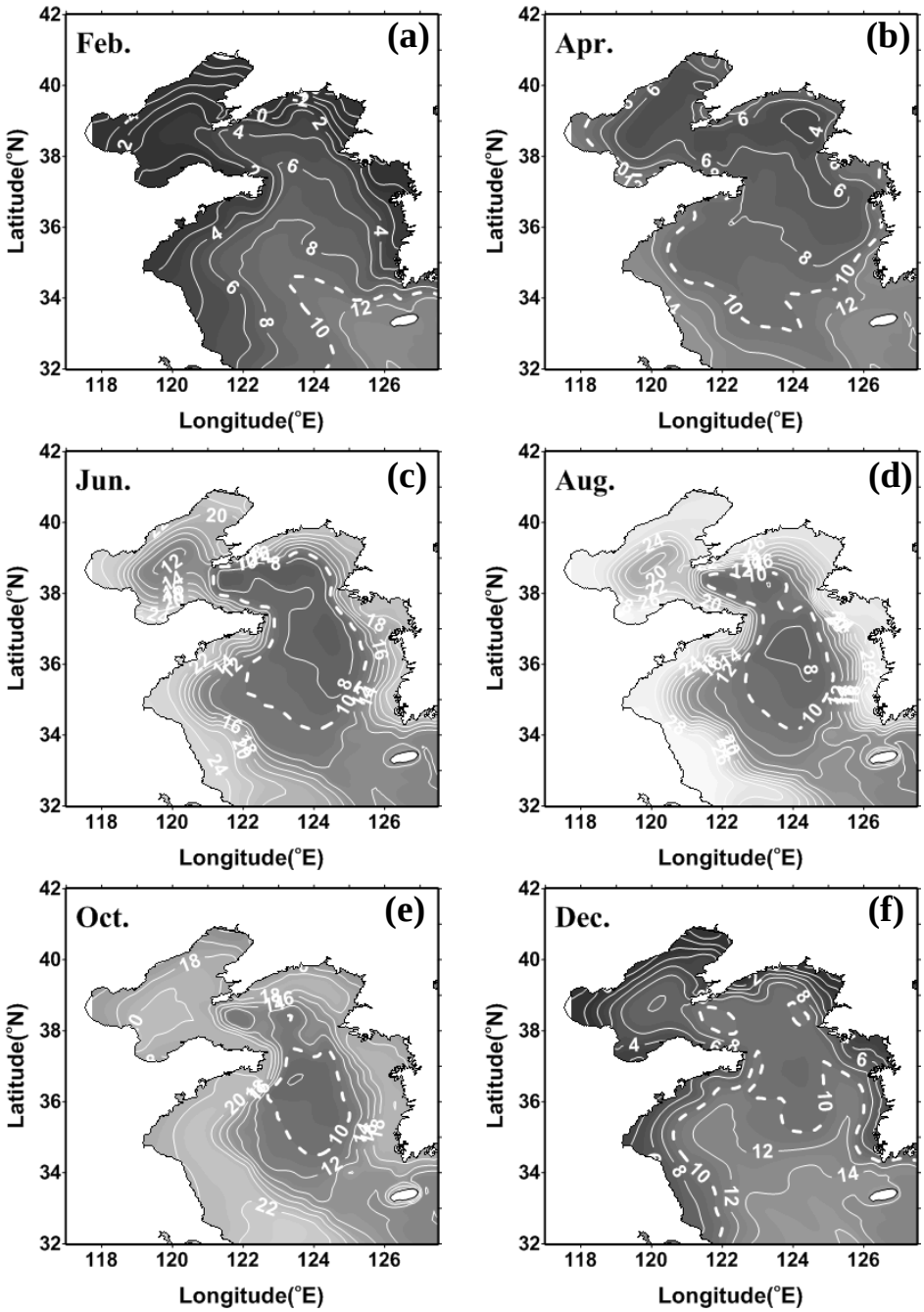

Figure 3. Monthly mean temperature distributions at bottom (or 75 m depth where is deeper than 75 m) of model result (℃) (a) February (b) April (c) June (d) August (e) October (f) December.

3. Result

3.1 Inter-annual variation of the southern limit

It is important to understand the location of the YSBCW in summer, because it is crucial to determine physical and biogeochemical properties in the YS [Zhang et al., 2008]. Figure 4a shows the 30 years mean vertical temperature distribution in August along the observation station (Figure 1) on deep trough. White line is 10℃ isothermal line. Sea surface temperature is more than 25℃, but cold water less than 10℃ appears near the bottom. South locations of 10℃ isothermal line are investigated during the 30 years. In order to explore the inter-annual variability of the location of the YSBCW, the southern limit of the YSBCW is defined as the distance of 10℃ isothermal line from the observation line 307 by NFRDI along the sea floor. The observation shows a large inter-annual variation of the YSBCW southern limit during the last 30 years (Figure. 4b). The YSBCW southern limit retreats to the north or extends to the south from year to year. The maximum and minimum distances are found at 422 km in 1984 and at 146 km in 1991, respectively. Because the YSBCW is formed during the previous winter, bottom temperature in summer is closely related with the sea surface temperature of the previous winter [Kang et al., 1987].

Numerical models can indicate the entire distribution of the YSBCW and well describe its dynamical interactions with the causes [Riedlinger et al., 2000]. In

order to overcome the limitations associated with the sparse spatial and temporal samplings in the observation data, numerical model results are analyzed. Bottom temperature distribution of model result in August of each year during the 30 years show detail inter-annual variation of the YSBCW (Appendix Figure 4). Southern limits of model result are calculated using the monthly mean bottom temperature at the same location as the observation. The simulated southern limit agrees with the observed variability reasonably well (Figure 5). Although, the details of the variability differ quantitatively, the overall change of the meridional migration of the southern limit is well captured.

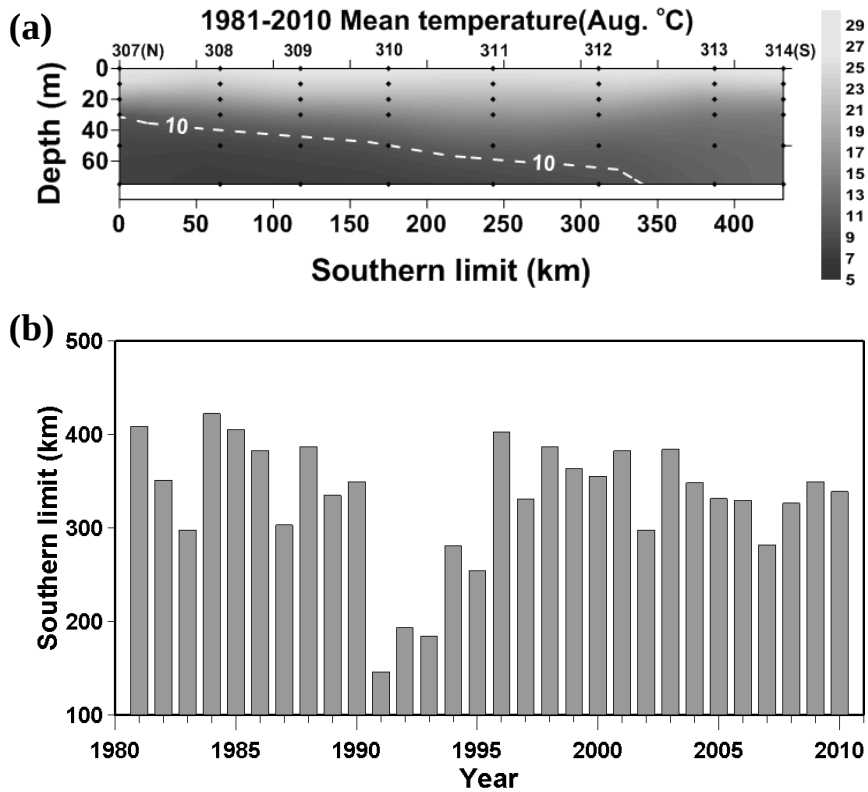

Figure 4. (a) Mean vertical meridional section of temperature along the observation stations (Figure 1) and (b) Southern limit during 30 years (1981-2010) of observation data in August by NFRDI.

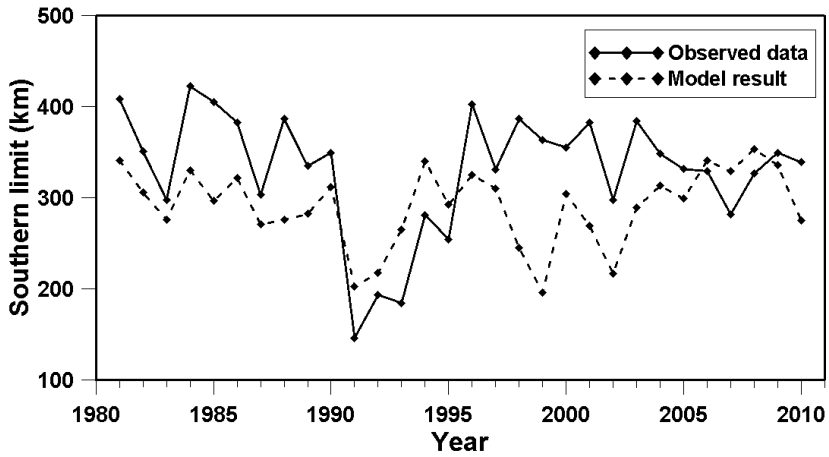

Figure 5. Southern limits of numerical model result and observation data in August from 1981 to 2010.

3.2 Correlation with the SST in the previous winter

An anomalously cold of the YSBCW in 1981 might be related to cooling of the sea surface during the previous winter [Yang et al., 1984]. To explore the relation between the southern limit variability and the oceanic condition of the previous winter, correlation between February SST and the southern limit in August was calculated (Figure 6).

Figure 6a and b show the analysis of the observed data and model result, respectively. Correlation coefficient of the observed data between the August southern limit and the February SST is -0.612 during the 30 years (Significant at a 95% confidence level, $r > 0.341$). This negative correlation means that higher SST in February tends to lead the YSBCW to a less southward spread at depths. Linear regression suggests that the southern limit is reduced by about 54 km when the SST in February rises by 1℃. Figure 6b shows the correlation between the February sea surface temperature and the southern limit obtained from the model. Correlation coefficient is -0.767, which is higher than the observation-based estimate. Consistent with the observation, the model result also indicates that increased SST is associated with decreased southern limit in the following summer. Using a linear regression of the model results, we also find that an increase in air temperature of 1℃ tends to reduce the southern limit by about 49 km. This is about 54 km in the observation.

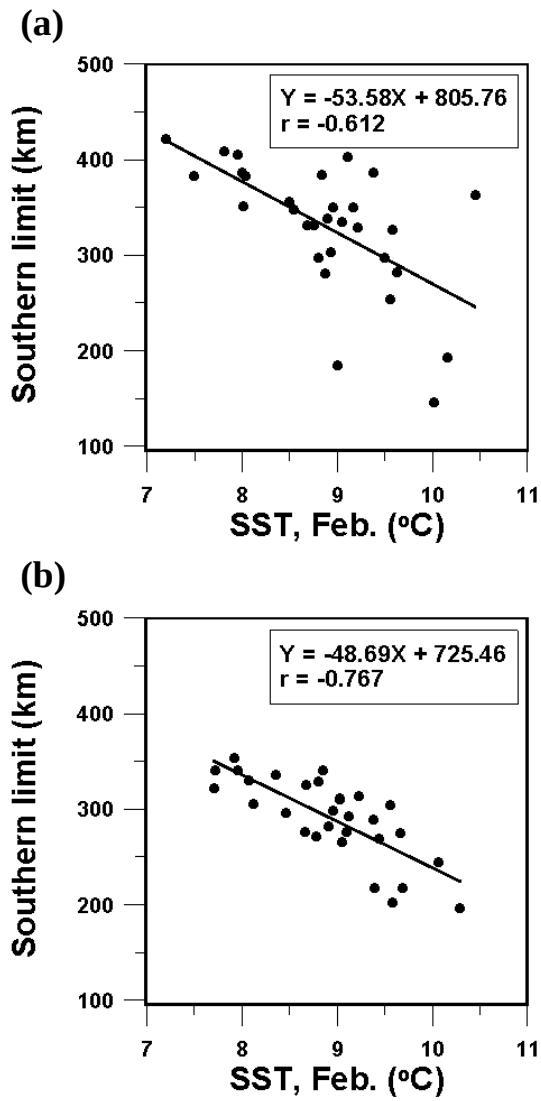

Figure 6. Correlation between sea surface temperature in February and southern limit of the Yellow Sea Bottom Cold Water in August. (a) observed data (b) model result.

3.3 Correlation with the southerly wind stress in summer

As first suggested by Park (1986), the YSBCW flows southward after it is formed in the northern YS [Zhang et al., 2008]. The evolution of the southern limit after its formation is an important factor controlling the variability of the location of the YSBCW. In order to reveal the inter-annual variations of the cold water displacement in summer, southern limits in August are compared with southern limits in June (Figure 7). Because the observation data is missing in June 2010, a comparison is done for only 29 years (1981~2009).

Figure 7a shows the observed southern limits in August and June. Of total 29 years, the August southern limit is farther south than the June southern limit for 11 years. This means that southern limit in August moves or extends to the south after June. Model results show that the August southern limit is greater than the June southern limit for only 7 years out of total 30 years (Figure 7 b). In August, the sea surface becomes warmer and the ocean becomes more stratified than in June. Therefore, it is difficult to explain the expansion of the southern limit in August by using the heat transport between the sea surface and the bottom layer. Previous studies suggest a role of summer wind on the further expansion of the YSBCW [Zhang et al., 2008; Jacob et al., 2000]. Model results by Jacobs et al. (2000) suggest that in summer southerly wind generates southward flow at the bottom: the sea level increases in the northern areas of the YS by the southeasterly summer winds. The file-up of surface waters in the north creates a pressure gradient from the north to the south and generates a southward flow at the bottom layer. In order

to explore the relationship between the displacement of the southern limit and summer wind stress for the last 30 years, we calculate differences between the southern limits in August and June, and estimate the correlation with V component wind stress in summer (Figure 7).

The simulated difference between the June and August southern limits is positively correlated with the summer southerly wind stress with a correlation coefficient of 0.529 (Figure 7b). This result proves that anomalously stronger southerly wind stress in summer tends to push the southern limit further south in August. The same calculation using the observed southern limit, however, shows a much reduced correlation with r=0.121 (Figure 7a). A possible cause for the low correlation includes the use of the ECMWF wind, which are the reanalysis model results. Nevertheless, the qualitative agreement suggests that the extension of the August southern limit may be intimately tied to the summer winds.

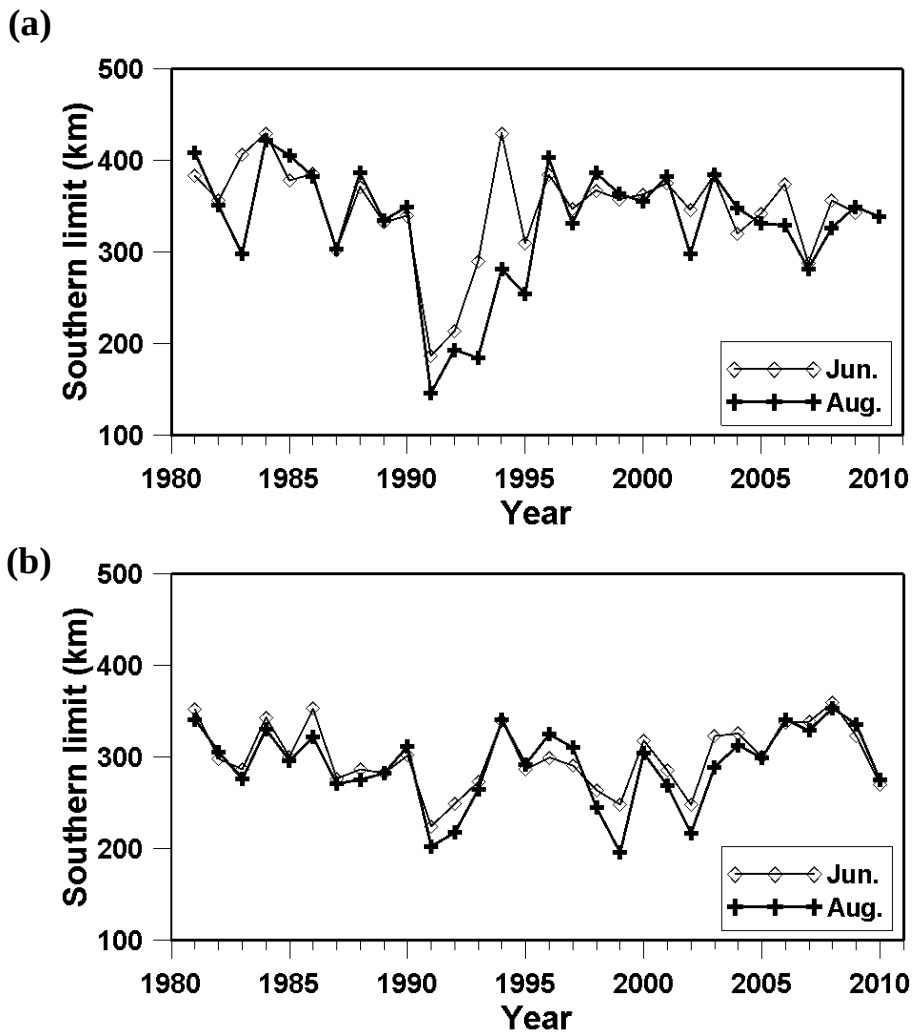

Figure 7. Southern limit of in June and August (a) observation data and (b) Model results during the 30 years.

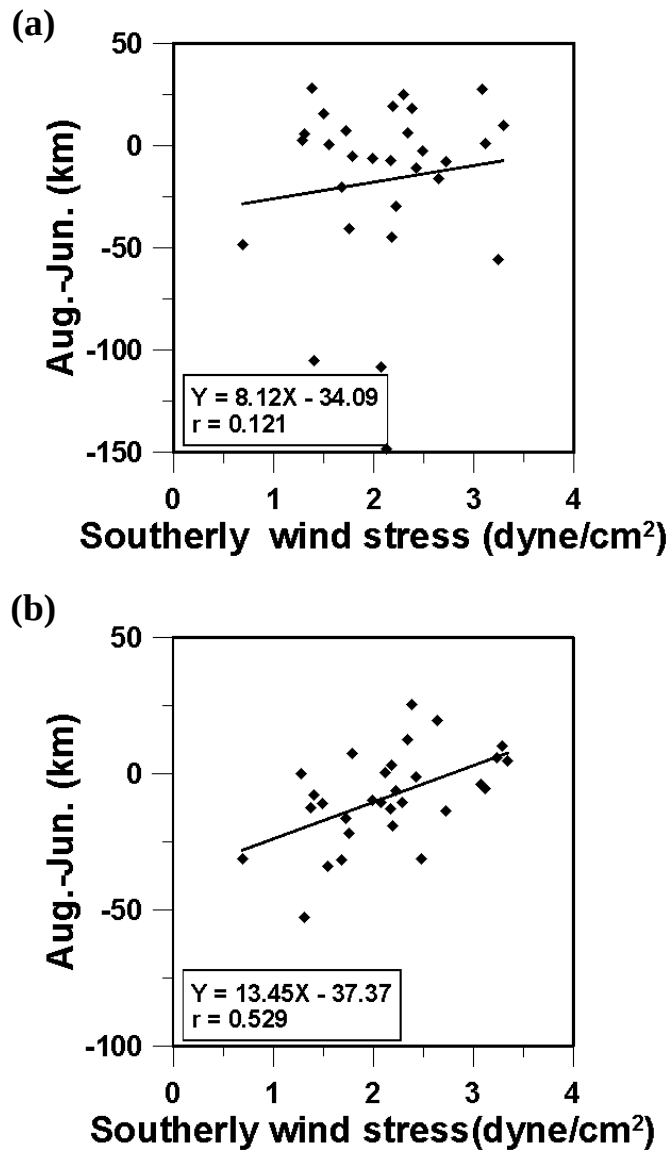

Figure 8. Correlation between southerly wind stress in summer and southern limit difference between in August and June. (a) Observation data (b) Model result.

3.4 Reconstructed southern limit based on the winter SST and summer wind

In the previous sections, we showed that the sea surface temperature in February and the summer wind stress both affect the extent of the southern limit of the YSBCW. In order to quantify how change in the southern limit is affected by two factors, we reconstruct the southern limit through a multiple regression analysis (Figure 9). The normal equation is

$$\text{Normal eq. of observation data} = -0.78\,\text{nSST} + 0.08\,\text{nWind} + 6.77 \quad (1)$$

$$\text{Nomal eq. of model result} = -1.07\,\text{nSST} + 0.39\,\text{nWind} + 8.70 \quad (2)$$

These equations suggest that SST in February has a greater impact than the summer wind stress in both the observation and model. Figure 9a shows the southern limit of observation data (solid line) and reconstructed southern limit (dashed line). The correlation coefficient is 0.614 and the southern limit variability is well captured by above two factors. Figure 9b compares the simulated southern limit (solid line) and the reconstructed southern limit (dashed line). The correlation coefficient in this case is as high as 0.808. Compared with the observation data, the

southern limit is explained better by both the winter air temperature and summer southerly wind stress.

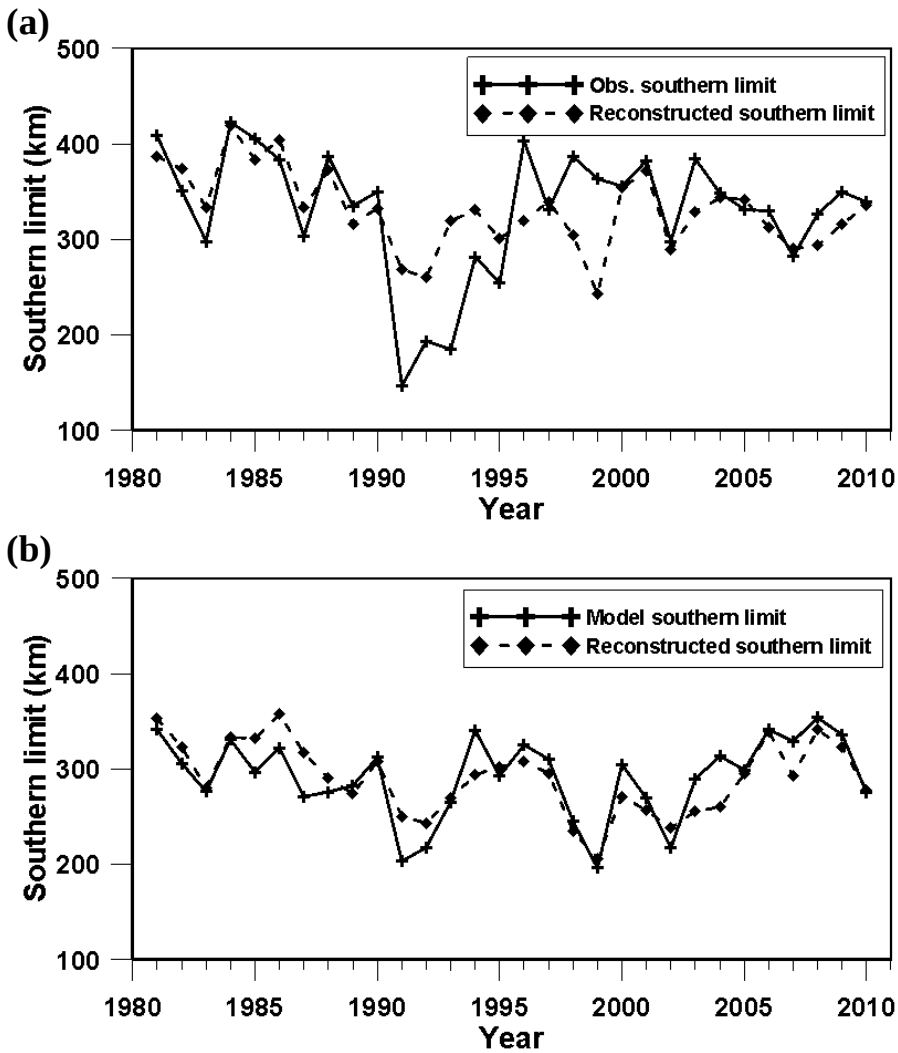

Figure 9. Reconstructed southern limit based on the sea surface temperature in February and southerly wind stress in summer. (a) Observation data (b) Model result.

4. Discussion

4.1 Effect of air temperature and wind on the SST in winter

The correlation analysis between the southern limit in August and SST in February reveals the importance of winter sea water temperature in setting the southern limit of the YSBCW in the following summer. In order to examine factors affecting SST in February, air temperature and wind speed in winter are analyzed.

Figure 10a and b show the correlation between February SST and winter air-temperature obtained from the observation and model. Both observed and simulated SSTs are positively correlated with air temperature in winter. This result suggests that anomalously high air temperature is associated with anomalously warm SST in winter. Through the influence on winter SST, winter air temperature is considered as an important factor controlling the locations of the YSBCW.

Previous studies identified two different roles played by winter wind stress. Kim et al., (1999) revealed that the strong northerly winds introduce a large vertical contrast between air temperature and SST, which produces a large amount of heat loss. On the other hand, the model result by Hsueh and Yuan (1997) showed that the increased sea level induced by the northerly strong monsoon generates inflow of warm and salty water in the south YS. This inflow warms the YSBCW in next summer. To explore the role of the winter winds, we plot a scatter diagram between

SST in February and winter wind speed (Figure 10c and d). The correlation coefficient from the model result is higher than observation data (r=0.305) by 0.522. This result shows that the stronger wind speed can decrease February SST. As a result, wind speed and air temperature in winter play crucial roles in temporal changes in the southern limit of the YSBCW.

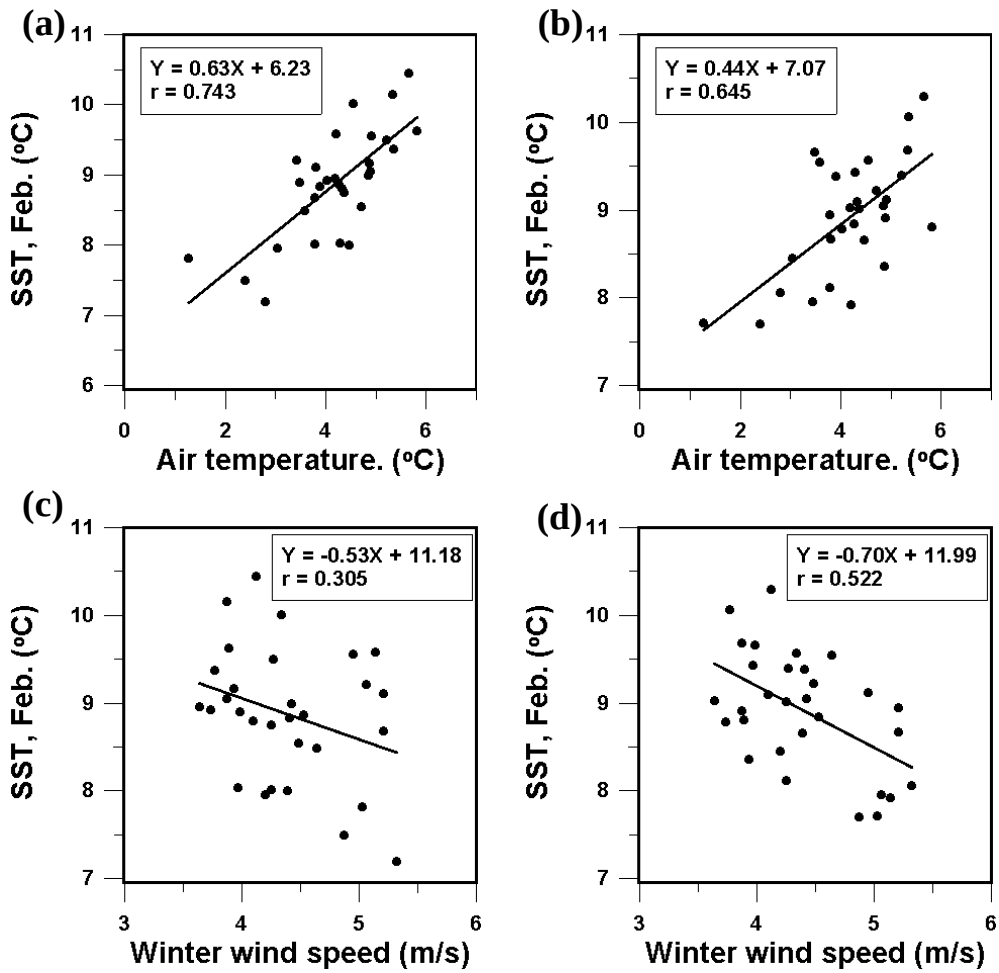

Figure 10. Correlation between SST in February and winter air temperature ((a) and (b)), and winter wind speed ((c) and (d)) during 30 years. (a) and (c) SST of the observation data , (b) and (d) SST of the model results.

4.2 Effect of the YSBCW temperature in the previous year on the SST in winter

Previous results suggest that the strong northerly wind and cold air cool the sea surface across a wide area. This winter cold water leads to the expansion of the southern limit. Figure 11 shows the relation between southern limit of model result and winter atmosphere conditions. This result implies that anomalously high SST in February is correlated with anomalously high winter air temperature and weak winter wind speed. However southern limit in 2007 did not follow this relation. The correlations of SST with the air temperature and wind speed in 2007 are analyzed to reveal the reason.

The southern limit in 2007 (about 329km) is extended more than the 30 years mean of about 291 km (Figure 12b and d). Summer southerly wind stress in 2007 (about 1.92 dyne/cm^2) was weaker than the 30 years mean value (about 2.08 dyne/cm^2). SST in February 2007 (about 8.9℃) was lower than the 30 years mean SST (about 9.1℃). Southern limit expansion in 2007 is due to the low SST in winter.

Although the low SST in winter, The winter air temperature in 2007 (about 5.81 ℃) was higher than the 30 years mean of about 4.18 ℃ and the wind speed in winter was weaker by 3.89 m/s relative to the 30 years mean of 4.39 m/s. This means that there may be other factors affecting SST in February besides winter air

temperature and wind speed.

In order to explain the cause, we analyzed previous year's bottom temperature in October. Because the YS in October is stratified, bottom water remembers the temperature and shape of the YSBCW in August. For this reason, Water temperature at 75 m depth in October is analyzed.

Figure 12a and c show the October temperature of 30 years mean (1980-2009) and 2006, respectively at 75m and bottom. The 30 years mean 10℃ isothermal line (Figure 12a) appears around stations of the observation line 311 (the southern limit is about 241 km)).

The 10℃ bottom temperature isothermal line in 2006 (Figure 12c) is located near the stations of observation line 313 (about 341 km) and it is located further south of the 30 years mean 10℃ isothermal line. The bottom water in 2006 is about 2 C° cooler than 30 years mean temperature. This result suggests that the initial cold bottom temperature (2006) before the winter atmospheric conditions affecting the ocean is associated with SST in winter and the southward expansion of the YSBCW. In order to explore the effect of the previous year's bottom water temperature on the winter ocean, correlation between SST in February and bottom water temperature in October is calculated (Figure 13). Figure 13a shows the scatter diagram between 75 m mean temperatures in previous October and February SST from the model. Correlation coefficient is as high as 0.430, and this result reveals that the warm temperature in October affects warm SST in February. The observed 75 m temperature in October has a correlation coefficient (0.307) with observed SST in February, which is lower than the model result. However, the relation between SST and sea water temperature in October suggests that winter

SST is affected by subsurface waters formed in a previous year.

The winter sea water, including the effect of previous year's ocean condition, remains on the bottom. Thus, previous year's bottom temperature is regarded as one of the factors affecting the southern limit of the YSBCW.

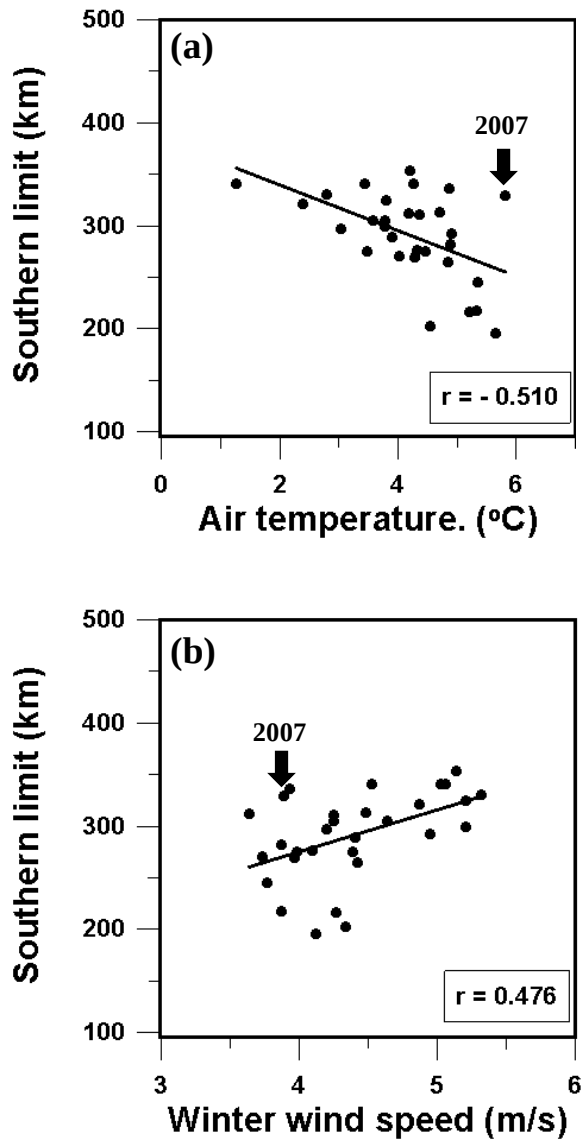

Figure 11. Correlation between southern limit of model result and (a) February air temperature (b) Wind speed in winter.

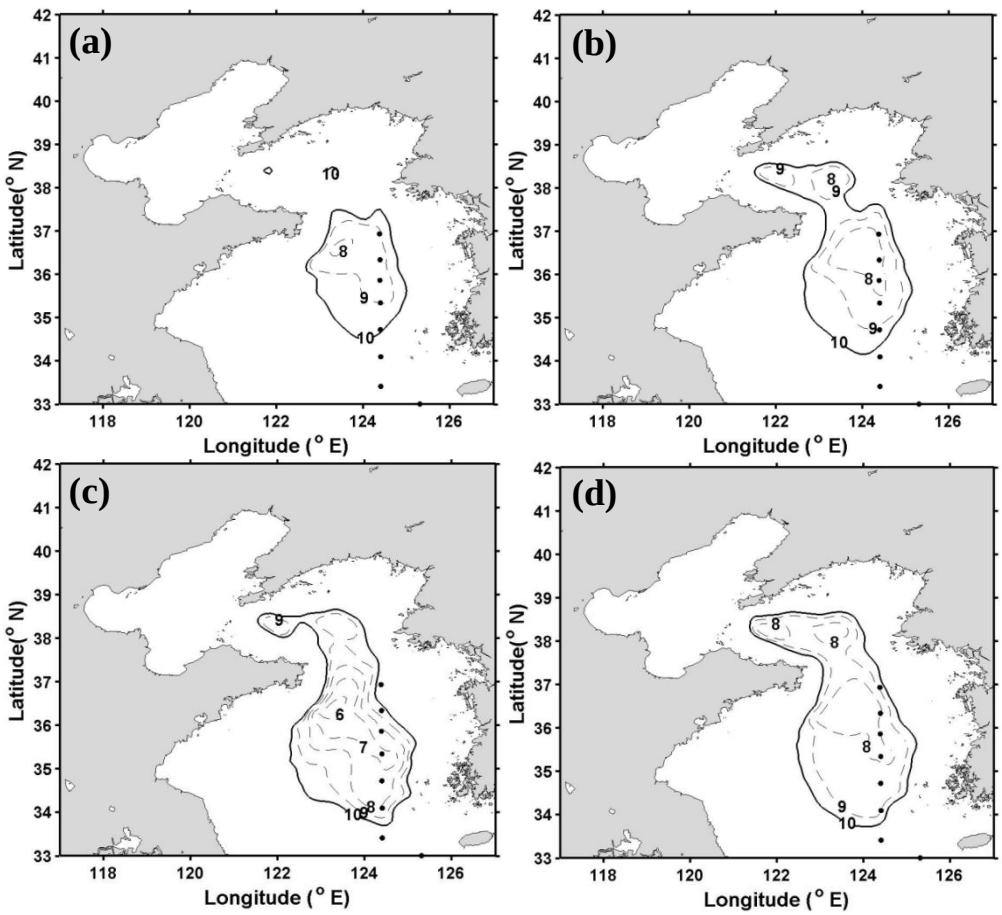

Figure 12. Horizontal temperature distributions at bottom (or 75 m depth where is deeper than 75 m) of model result (℃). During 30 years averaged temperature in October (a), and in August (b). Monthly mean temperature in October 2006 (c), and August 2007 (d). The black points on the figure represent the observation stations.

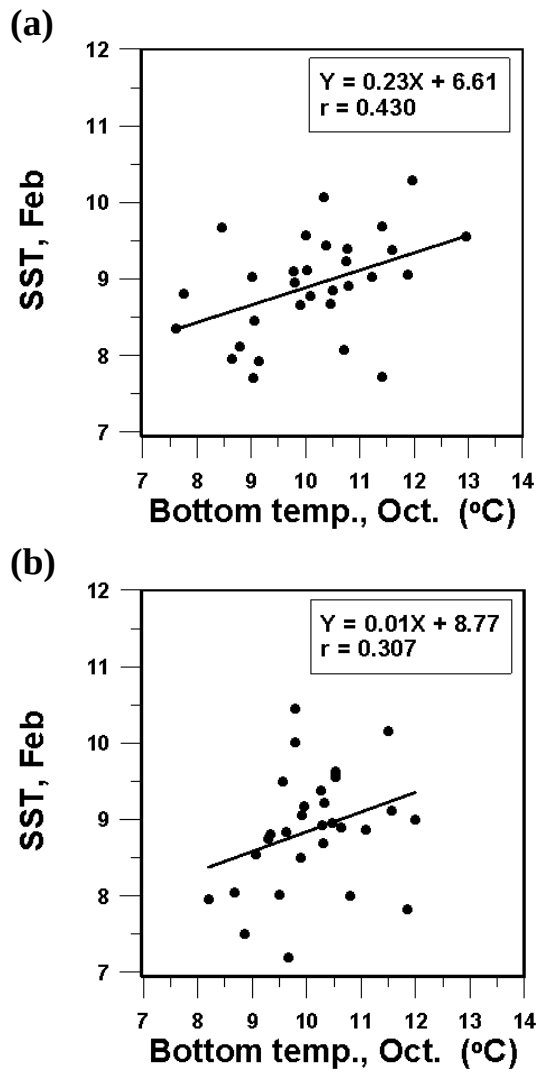

Figure 13. Correlation between 75 m water temperature in previous October and SST in February. (a) Model result (b) Observation data.

5. Conclusion

The southern limit of the YSBCW is defined as the distance of a 10℃ isothermal line from the observation line 307 by NFRDI. The southern limits obtained from the observation data and model show pronounced inter-annual variability over the last 30 years (1981-2010).

Both the model and observation show that sea surface temperature in February is negatively correlated with the southern limit. A correlation coefficient obtained from the observation data is -0.590 and from the model is -0.767.

To explore the southern limit variations during summer, southern limits in August and June are compared. For 11 years out of total 29 years, the observed southern limit is located further south in August than in June. On the other hand, model results show that the southern limits of 7 years during the 30 years are located further south in August than in June. The cause for the August expansion (relative to June southern limit locations) is the cold water displacement by summer southerly wind. Correlation between the southerly wind stress in summer and the departure of the simulated southern limit of the YSBCW in August is high (r=-0.529). This result shows that the southern limit in August tends to be more expanded than in June when the southerly winds are strong. However, a correlation coefficient between the observed southern limit and wind stress is low. Nevertheless, the southern limit expansion in August is found clearly in observation data as well as model result. Effect of summer wind stress can be better explained by the numerical model experiment.

Using the sea surface temperature in February and southerly wind stress in summer, we reconstructed the southern limits. A correlation coefficient between the reconstructed southern limit and the observed southern limit is 0.614, whereas a correlation between the reconstructed southern limit and the simulated southern limit is 0.808. The model result particularly shows that winter ocean environment and summer winds are crucial factors determining the locations of the southern limit.

There are two different views regarding the effect of winter wind stress. This study suggests that strong northerly winds cool the seawater, thereby influencing the extent of the southern limit.

This study also identified the importance of initial ocean condition (previous year's bottom temperature) before the winter cooling. We compared observed/simulated SST in February with 75m water temperature in previous October. Correlation coefficients between two factors are estimated to be 0.307 for observation and 0.430 for the model. This result suggests that the bottom temperature in the autumn affects sea surface temperature in the following winter. Along with summer wind stress, the winter sea surface temperature including air temperature, wind and previous year ocean condition is a crucial factor on the inter-annual variation in the southern limit of the YSBCW.

Appendix

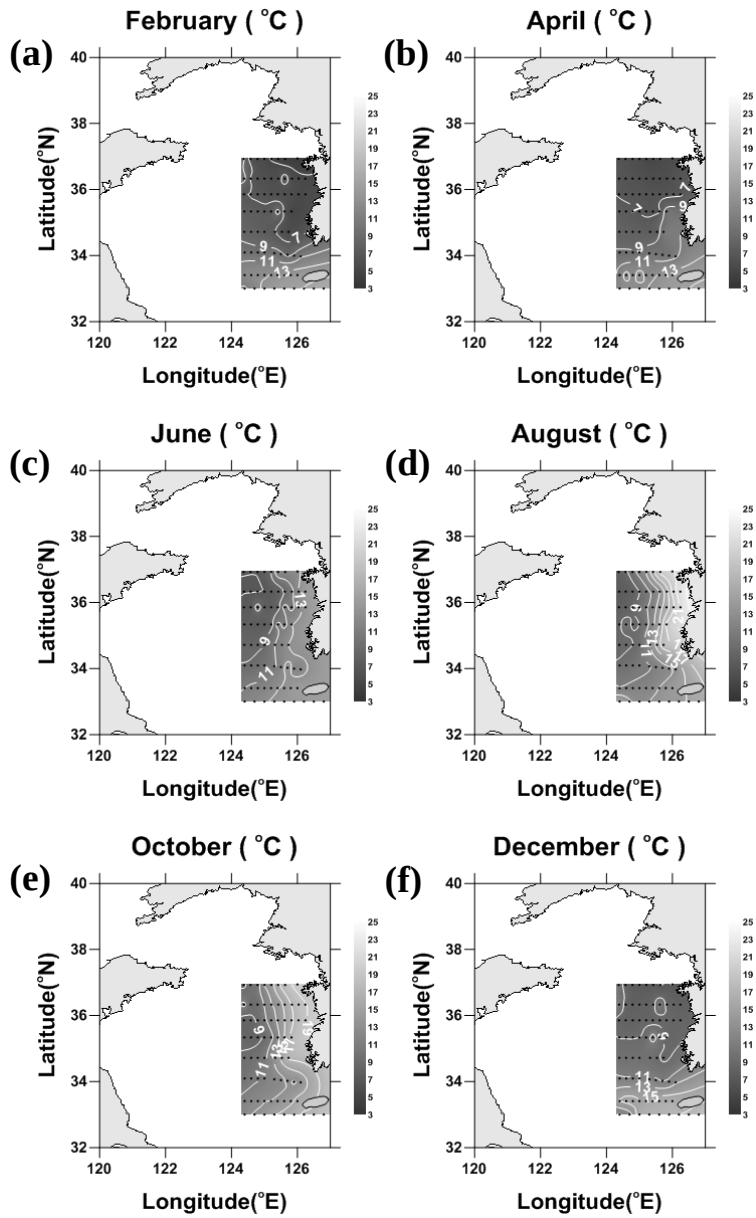

Figure A 1. Observed mean bottom temperature during 30 years by NFRDI. (a) February (b) April (c) June (d) August (e) October (f) December.

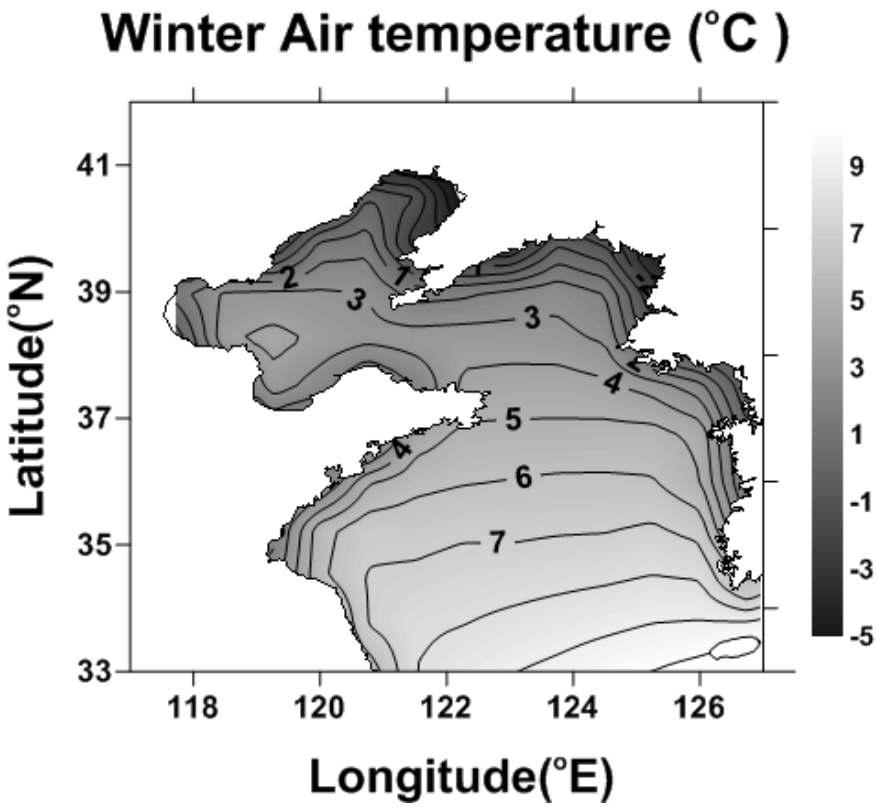

Figure A 2. Mean winter air temperature during 30 years by ECMWF.

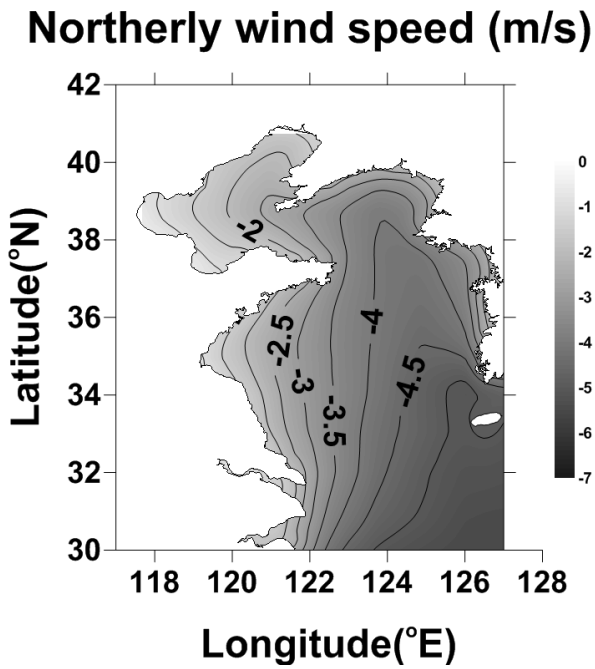

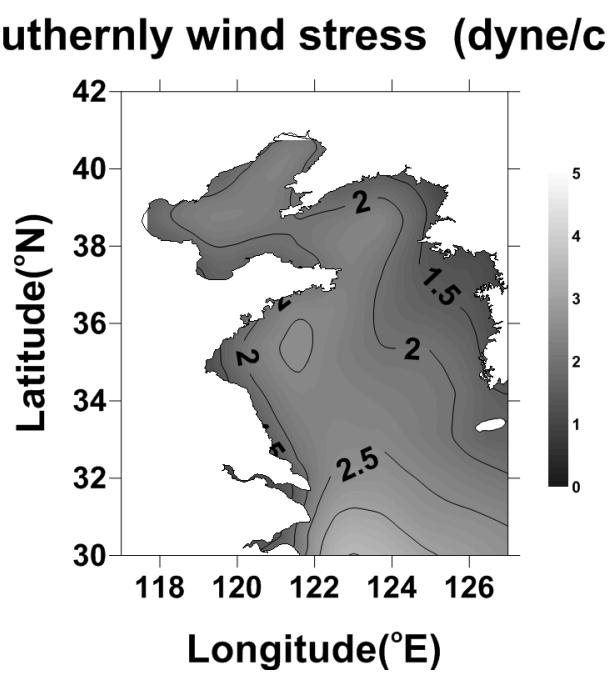

Figure A 3. (a) Mean northerly wind speed in winter and (b) mean southerly wind stress in summer during 30 years. Data are from ECMWF.

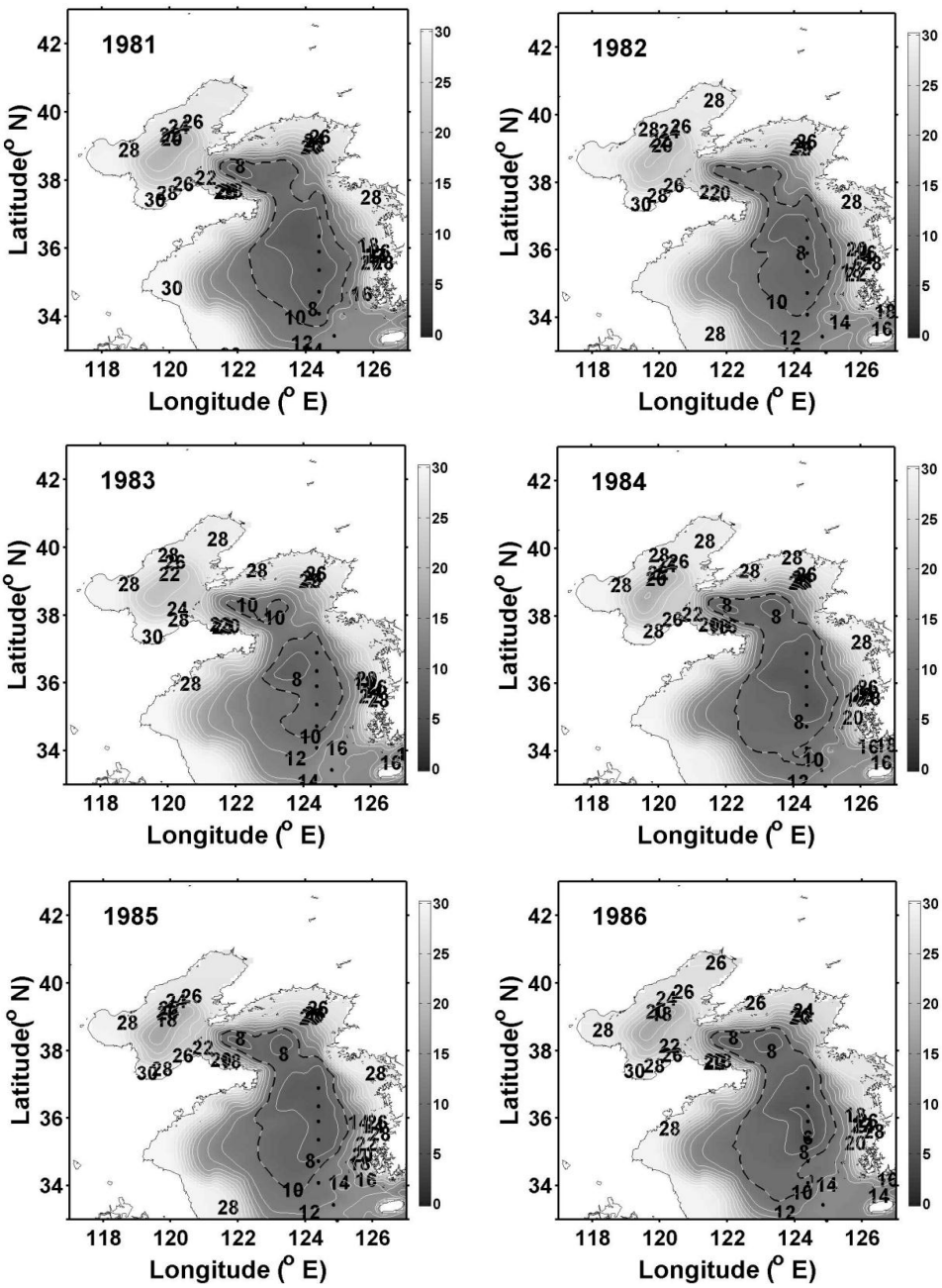

Figure A 4. Monthly mean temperature distributions at bottom (or 75 m depth where is deeper than 75 m) of model result (℃) in August during 30 years.

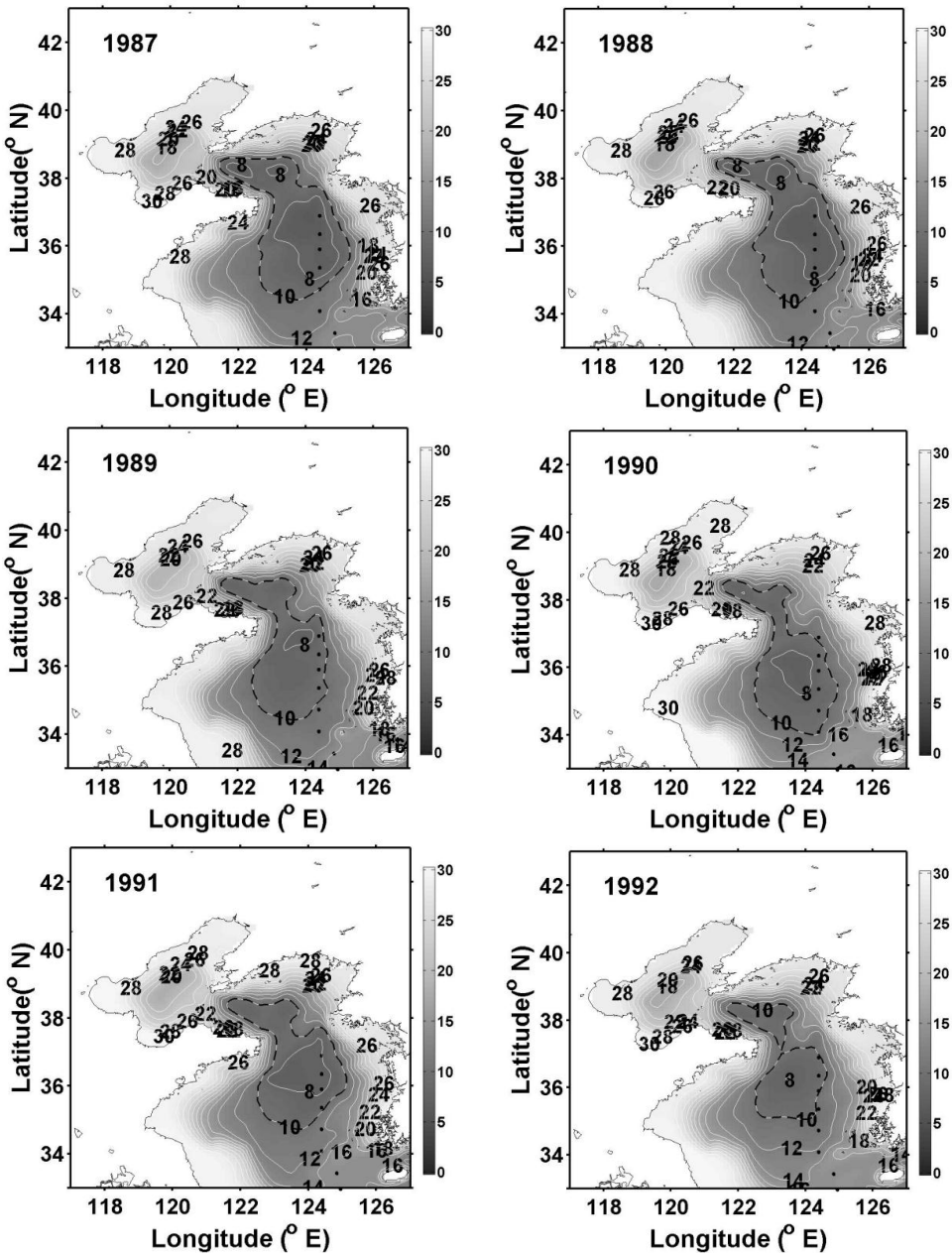

Figure A 5. (continued)

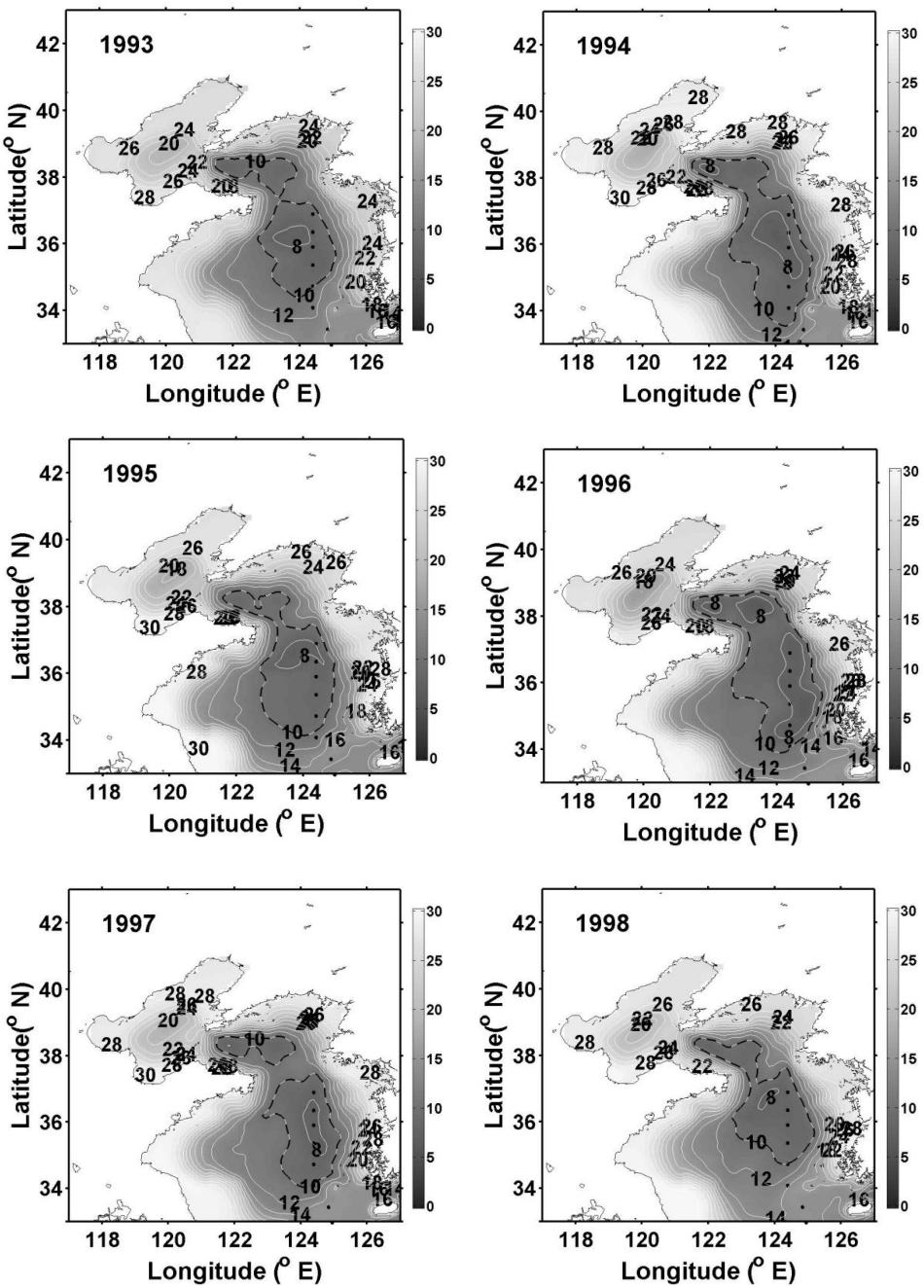

Figure A 6. (continued)

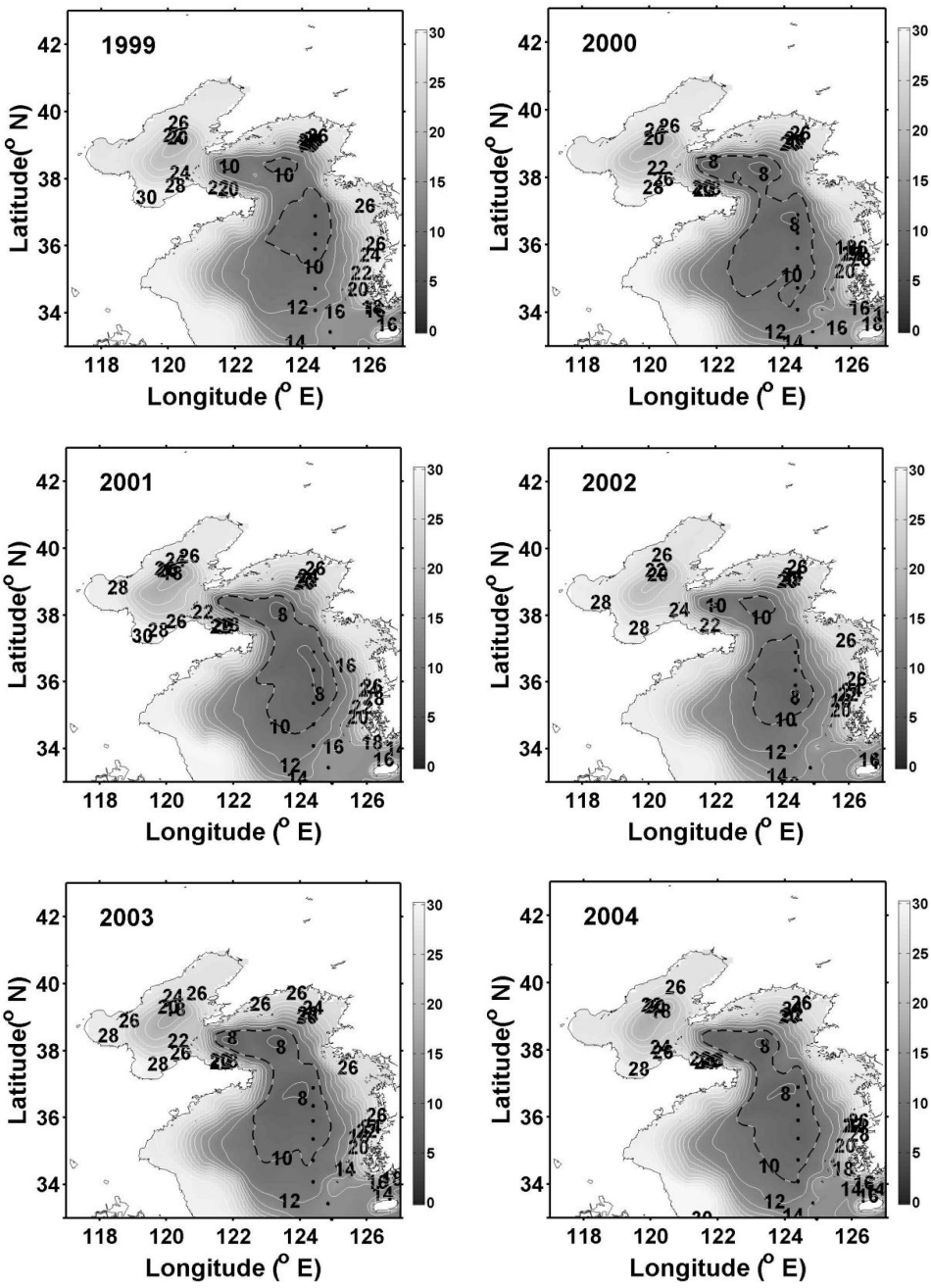

Figure A 7. (continued)

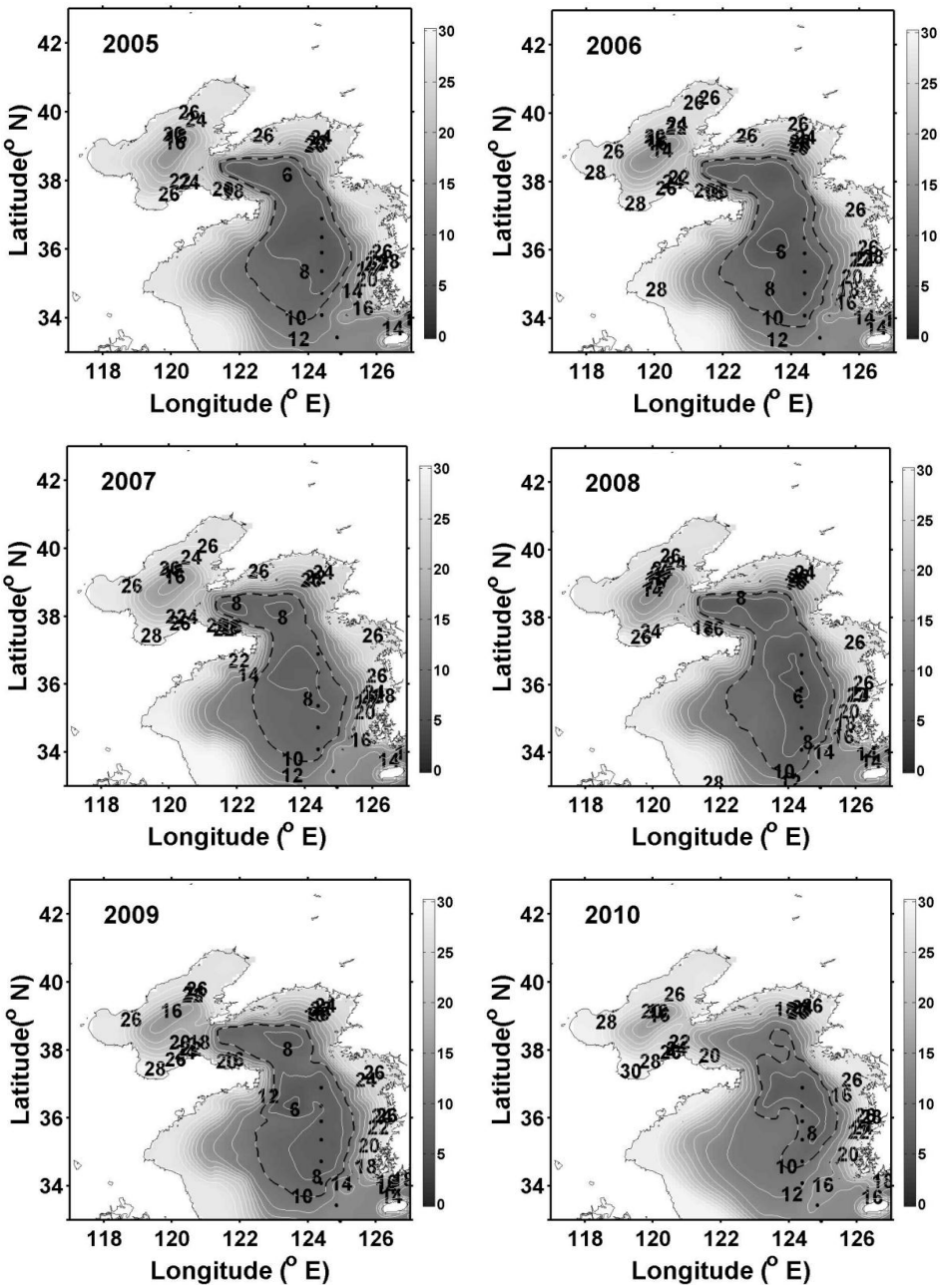

Figure A 8. (continued)

References

Cho, Y.-K., Seo, G. H., Choi, B.-J., Kim, S., Kim, Y. G., Youn, Y. H., and Dever, E. P. (2009). Connectivity among straits of the northwest Pacific marginal seas.*Journal of Geophysical Research, 114*(C6), C06018.

Cho, Y.-K., Seo, G. H., Kim, C. S., Choi, B.-J., and Shaha, D. C. (2013). Role of wind stress in causing maximum transport through the Korea Strait in autumn.*Journal of Marine Systems*. 115:33-39.

Dunxin, H., and Qingye, W. (2004). Interannual variability of the southern Yellow Sea cold water mass. *Chinese Journal of Oceanology and Limnology, 22*(3), 231-236.

Egbert, G. D., and Erofeeva, S. Y. (2002). Efficient inverse modeling of barotropic ocean tides. *Journal of Atmospheric and Oceanic Technology*, *19*(2), 183-204.

Fairall, C. W., Bradley, E. F., Rogers, D. P., Edson, J. B., and Young, G. S. (1996). Bulk parameterization of air-sea fluxes for tropical ocean-global atmosphere coupled-ocean atmosphere response experiment. *Journal of Geophysical Research*, *101*(C2), 3747-3764.

Guan, B. X. (1963). A preliminary study of the temperature variations and the characteristics of the circulation of the cold water mass of the Yellow Sea.*Oceanologia et Limnologia Sinica*, *5*(4), 255-283.

Hsueh, Y., and Yuan, D. (1997). A numerical study of currents, heat advection, and sea-level fluctuations in the Yellow Sea in winter 1986. *Journal of physical oceanography*, *27*(11), 2313-2326.

Hur, H. B., Jacobs, G. A., and Teague, W. J. (1999). Monthly variations of water masses in the Yellow and East China Seas, November 6, 1998. *Journal of Oceanography*, *55*(2), 171-184.

Jacobs, G. A., Hur, H. B., and Riedlinger, S. K. (2000). Yellow and East China Seas response to winds and currents. *Journal of geophysical research*,*105*(C9), 21947-21.

Kang, Y. Q., and Kim, H. K. (1987). Relationships between the winter-time surface water temperature and the summer-time bottom water temperature in the West Sea of Korea. *J. Ocean. Soc. Korea*, *22*, 228-235.

Kim, Y. S., and Kimura, R. (1999). Estimation of the Heat Flux Exchange between the Air-Sea Interface over the Neighbouring Seas of Korean Peninsula.*J. Korean Meteor. Soc*, *35*(4), 501-510.

Mellor, G. L., and Yamada, T. (1974). A hierarchy of turbulence closure models for planetary boundary layers. *Journal of the Atmospheric Sciences*, *31*(7), 1791-1806.

Park, S., Chu, P. C., and Lee, J. H. (2011). Interannual-to-interdecadal variability of the Yellow Sea Cold Water Mass in 1967–2008: characteristics and seasonal forcings. *Journal of Marine Systems*, *87*(3), 177-193.

Park, Y. H. (1986). Water characteristics and movements of the Yellow Sea Warm Current in summer. *Progress in oceanography*, *17*(3), 243-254.

Riedlinger, S. K., and Jacobs, G. A. (2000). Study of the dynamics of wind-driven transports into the Yellow Sea during winter. *Journal of Geophysical Research: Oceans (1978–2012)*, *105*(C12), 28695-28708.Wang, R., Zuo, T., and Wang, K. E. (2003). The Yellow Sea cold bottom water—an oversummering site for Calanus sinicus (Copepoda, Crustacea). *Journal of Plankton Research*, *25*(2), 169-183.

Teng, S.K., Yu, H., Tang, Y., Tong, L., Choi, C.I., Kang, D., Liu, H., Chun, Y., Juliano, R.O.,Rautalahti-Miettinen, E., and Daler, D., 2005. Global international waters assessment: Yellow Sea. GIWA Regional Assessment, 34. University of Kalmar, Sweden.

Xia, C., Qiao, F., Yang, Y., Ma, J., and Yuan, Y. (2006). Three-dimensional structure of the summertime circulation in the Yellow Sea from a wave-tide-circulation coupled model. *Journal of Geophysical Research: Oceans (1978–2012)*, *111*(C11).

Yang, S.-K., Cho, K.-D., and Hong, C.-H., 1984. On the abnormal low temperature phenomenon of the Yellow Sea Bottom Cold Water in Summer, 1981. *Journal of the oceanological Society of Korea*, 19(2), 125-132.

Zhang, S. W., Wang, Q. Y., Lü, Y., Cui, H., and Yuan, Y. L. (2008). Observation of the seasonal evolution of the Yellow Sea Cold Water Mass in 1996–1998.*Continental Shelf Research*, *28*(3), 442-45

요 약

황해저층냉수(YSBCW)는 여름철 해수 표면의 가열로 형성되는 수온약층 아래 존재하는 수온 10℃ 이하 수괴를 말한다. 본 연구에서는 황해저층냉수의 남쪽 한계에 대하여 정의 하고, 남쪽 한계의 연 변화에 영향을 미치는 요인들에 대하여 살펴보았다.

국립수산과학원에서 제공하는 서해의 정선관측 자료 중 가장 외해 정점(10번)의 8월 수온을 1981년부터 2010년까지 분석하였다. 관측 자료에서 가장 북쪽 관측선인 307 관측선으로부터 75m 10℃ 등온선의 남쪽으로 거리를 황해 저층냉수의 남쪽 한계로 정의 하였다. 관측값의 남쪽한계는 30년 동안 큰 연변화를 하는 것으로 나타났다. 관측 자료의 오차와 공간적 해상도에 따른 한계를 보완하기 위해 수치모델결과를 분석하혔다. 모델의 저층냉수 남쪽 한계는 관측값과 변화 양상이 유사하게 재현되었다.

2월 표층 수온과 8월 남쪽 한계는 관측값과 모델 결과 모두 높은 상관관계를 보였으며 표층수온이 감소 할수록 남쪽한계는 더 남쪽에 형성됨을 알 수 있다.

30년간 8월과 6월의 남쪽 한계를 비교한 결과 특정 해 8월 남쪽한계가 6월 남쪽 한계보다 남쪽에 형성됨을 알 수 있었다. 이는 여름철 남풍에 의하여 8월 남쪽 한계가 확장된 것으로 생각된다.

겨울철 강한 북풍은 겨울철 기온과 함께 해수 표층의 열손실을 만든다. 차가워진 겨울철 해수는 다시 여름철 저층냉수의 남쪽 한계 확장에 영향을 미친다.

기존에 밝혀진 요인들 외에 전 해의 해양 환경이 저층냉수에 영향을 주는 것으로 나타났다. 전 해 10월 저층 수온과 다음에 8월 저층냉수의 관계는 관측과 모델 결과 모두에서 양의 상관관계를 보여 주었다.

주요어 : 황해, 수온, 황해저층냉수, 연변화, 표층 수온, 기온, 바람 응력

학 번 : 2011-23266